iScience

Article

# Adaptive cross-country optimization strategies in thermal soaring birds

## Graphical abstract

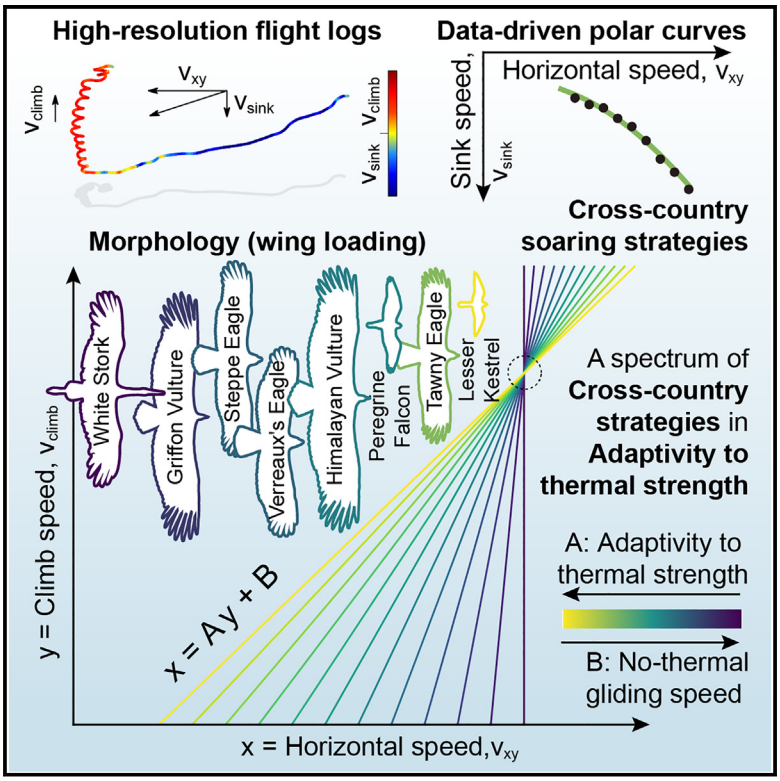


## Highlights

- Comprehensive GPS dataset of thermal soaring birds validates aerodynamic theory
- Cross-country strategy links gliding speed to thermal strength (climb rate)
- Species apply a range of strategies that vary in thermal strength adaptation
- Birds with lower wing loading show higher adaptivity to thermal strength

## Authors

Göksel Keskin, Olivier Duriez, Pedro Lacerda, Andrea Flack, Máté Nagy

## Correspondence

mate.nagy@ttk.elte.hu

## In brief

Ecology; Zoology; Ornithology; Evolutionary ecology

Keskin et al., 2025, iScience *28*, 112090
March 21, 2025 
https://doi.org/10.1016/j.isci.2025.112090

CellPress

iScience

CellPress
OPEN ACCESS

Article

# Adaptive cross-country optimization strategies in thermal soaring birds

Göksel Keskin,[1,2] Olivier Duriez,[3] Pedro Lacerda,[1,2] Andrea Flack,[4] and Máté Nagy[1,2,5,6,7,*]
[1]MTA-ELTE Lendület Collective Behaviour Research Group, Hungarian Academy of Sciences, Budapest, Hungary
[2]Department of Biological Physics, ELTE Eötvös Loránd University, Budapest, Hungary
[3]CEFE, University Montpellier, CNRS, EPHE, IRD, Montpellier, France
[4]Collective Migration Group, Max-Planck Institute of Animal Behavior, Konstanz, Germany
[5]Max-Planck Institute of Animal Behavior, Konstanz, Germany
[6]Senior author
[7]Lead contact
*Correspondence: mate.nagy@ttk.elte.hu
https://doi.org/10.1016/j.isci.2025.112090

## SUMMARY

Thermal soaring enables birds to perform cost-efficient flights. Although aerodynamic rules dictate the costs of flight, soaring species vary strongly in their morphologies and behavioral strategies. To quantify morphology-related differences in behavioral cross-country strategies, we analyzed a large dataset consisting of over a hundred individuals from 12 soaring species recorded with high-frequency tracking devices. We quantified their performance during thermalling and gliding flights and their overall cross-country behavior. Our results confirmed aerodynamic theory across the species; species with higher wing loading typically flew faster and consequently turned on a larger radius than lighter ones. Furthermore, the combination of circling radius and minimum sink speed determines the maximum benefits soaring birds obtain from thermals. Notably, we observed a spectrum of strategies regarding the adaptivity to thermal strength and uncovered a universal rule for cross-country strategies for all analyzed species which can provide inspiration for technical applications, like autopilot for robotic gliders.

## INTRODUCTION

Flying is energetically costly but many species have adapted their morphology and behavior to cope with the different requirements of this aerial lifestyle. Large, heavy bird species have developed energy-efficient flight modes, such as soaring-gliding flight[1,2] because the energetic costs of flapping wings increase with body mass.[3–5] The aerodynamic theory behind soaring is well established, and soaring birds exhibit a strong ecological, behavioral, and morphological diversity[6] (Table S1 and S2).

During soaring, birds gain altitude when circling in thermal convective updrafts (commonly referred to as thermals: localized regions of rising, buoyant air heated by sunlight[7,8]). Thermalling is followed by gliding flight (inter-thermal flight), where birds descend while traveling horizontal distances.[9,10] During this gliding phase, birds can adjust their gliding angle (i.e., steepness of the descending glide) which determines their horizontal (gliding) airspeed and their vertical (sinking) speed. This relationship is also known as the glide polar.[11,12] Previous studies have shown that the performance of a glider (bird or aircraft) depends strongly on its wing shape.[11,13–15] For example, species with long, narrow wings (high aspect ratio wings) can be more efficient at gliding with their higher lift to drag ratio, while species with higher wing loading (ratio between body mass and wing area) can achieve increased flight speed.[6,15,16] More specifically, (1) the horizontal speed that ensures the maximal horizontal travel distance from a given height depends ($V_{xy}^{Best\ Glide}$) on the wing loading,[16] (2) the glider's lift to drag ratio is a function of the wing's aspect ratio,[12,17] and (3) its turning radius during thermalling is directly proportional to wing loading.[12] Thus, all these morphological factors drive flight performance but disentangling the importance of each factor separately and for different species is challenging.

Previous studies of soaring flight used motor gliders,[4,18] radars,[8,19–21] or multi camera videography techniques[22–24] to examine the flight performance of free-flying birds. Currently modern bio-logging techniques allow us to obtain not just high-precision measurements of the birds' positions and movements in three dimensions but enable us to accurately measure the morphological features of each individual bird and species when attaching the devices.[25–29] Here, we compiled a large tracking dataset, that contains detailed flight records of 12 bird species, belonging to 5 families with different lifestyles (*Accipitridae*, *Cathartidae*, *Falconidae*, *Threskiornithidae*, and *Ciconiidae*; species details in Table S1). The dataset includes scavengers (3 [old-world] vultures and 1 [new-world] condor that look for food on the ground from high flight height), predators (searching for mobile prey that attack in the air [1 large falcon], on the ground [3 eagles], or at water surface [1 sea eagle]), and three species foraging on insects or small mammals that migrate

long distances (1 small falcon, 1 stork, and 1 ibis). Despite these behavioral differences, all species rely heavily on soaring flight and most have broad, elongated wings (relative to their body mass) with relatively similar aspect ratios (between 6.27 and 8.46). In addition, they differ in wingspan, wing loading and body mass (by almost two orders of magnitude, see Table S2), likely generating interspecific variations in flight behavior.[6,30] Although our main goal is to compare different species, we also investigated individual trajectories of *Gyps fulvus*, where the large number of tracked individuals allowed us to examine intraspecific variations in flight behavior and compare them with the general species-level findings.

We compared the soaring and gliding behaviors of the different species by focusing on the performance and optimization of cross-country flights under different thermal conditions. We quantitatively characterized the species' flight performance and cross-country optimization strategies and compared the experimental results to the theoretical expectations of Pennycuick's flight tool[12] and the MacCready theory.[31] The MacCready theory states that the best speed during inter-thermal flight is indicated by the glide polar based on the expected climb rate of the upcoming thermal. In our interpretation, gliders aim to cover a given horizontal distance by series of gliding and thermalling in the shortest possible time.[31,32] We note that neither MacCready theory nor the present analyses consider geographical or topographical factors. We explored the potential use of three cross-country strategies that are optimized for different goals: (1) a strategy based on MacCready's theory that guarantees a maximal cross-country speed by adjusting gliding (horizontal) speed to thermal strength (ascending speed) according to the species' respective polar curve; (2) a strategy that maximizes travel distance from a given height using a gliding speed independent of thermal strength (i.e., choosing a horizontal speed corresponding to the best glide); or (3) a mixed strategy that combines the previous two. We predict that most species adapt their cross-country strategies according to the prevailing thermalling conditions.[32,33] A previous study, using a similar comparative approach, explored how gliding airspeed relates to the species' morphology while also testing whether this relationship also depends upon the risk of not finding a new thermal.[21] Yet, their flight data came from radar tracks only, without detailed individual morphological variations. In addition, their framework relied heavily on Pennycuick's equations[12] and could not cope with birds behaving outside of the expected optimal range (which could be very narrow in the case of weak thermals). Thus, here using high-frequency flight recordings, we tested the validity of these previous theoretical predictions from Pennycuick to then analyze cross-country strategies based on observed flight parameters (Figure 1).

## RESULTS

### Empirical and theoretical glide polar curves

To determine how these foraging specializations (e.g., aerial foragers vs. large, heavy scavengers; see Table S1) and the connected morphological differences (Table S2) relate to the gliding performance of these different species, we first created empirical (effective and observed) polar curves of the 12 species using high-frequency GPS trajectories during soaring-gliding flight, which also may include occasional or even frequent flapping bouts, following a second-order approximation[32] ($f(x) = ax^2 + bx + c$) (Table S1 and Supplementary Dataset; Figure S1). Note that Griffon vultures (*G. fulvus*) data originated from two different sources: (1) free-flying adults that were raised in captivity and trained with falconry techniques[35] and (2) free-flying wild birds of various ages.[36] The two datasets provided distinctive polar curves (mean absolute difference = 0.66 m/s, $p = 0.64$) which is why we decided to analyze them separately.

First, we experimentally validated previous theoretical approximations by examining how similar the empirical, data-based polar curves (although those may include flapping bouts as well) are to the polar curves resulting from Pennycuick's equations using the default flight tool settings for each species (i.e., default curves from Flight software, version 1.25; https://booksite.elsevier.com/9780123742995/).[12] We first noticed that these species-specific Pennycuick polar curves were similar between each species. To quantify the similarity, we calculated the mean absolute difference of the glide polars and found little variation between the species (mean = 0.09 m/s, standard deviation [SD] = 0.05 m/s, Figure S2A). Moreover, the polar curves based on Pennycuick's flight tool with default values (default curves) did not fit well the empirical data (Figure S2B). The mean absolute difference between the default curves and observed data points was not smaller compared to what was expected by chance when comparing to polar curves of different species ($\langle\Delta_{default}\rangle = 0.98$ m/s, $n = 12$, randomization test, $p = 0.5581$, Figure S2B). Although Pennycuick also suggested that these formulas should not be used with the default parameter settings,[12] many research studies only rely on the default values.[37–47] Thus, we searched the literature[12,48,49] for more realistic physical properties of the different species (i.e., the body drag coefficient, wing profile coefficient, and maximum lift coefficient). Using these updated parameters (shown in Table S3) the estimated glide polars ("improved" Pennycuick curves) became more diverse between the species (larger difference between the curves: mean = 0.24 m/s, SD = 0.14 m/s, Figure S2A) and more similar to the observed data points ($\langle\Delta_{improved}\rangle = 0.47$ m/s) but still did not fit significantly better than what was expected by chance ($n = 12$, randomization test, $p = 0.5547$). Yet, the empirical curves provided significantly better fit to the observed data points ($\langle\Delta_{empirical}\rangle = 0.19$ m/s, $n = 12$, randomization test, $p = 0.0488$) with a large variation between the species (difference between the curves: mean = 0.58 m/s, SD = 0.27 m/s, Figure S2A) which is why we used those for the remaining analyses.

Two main parameters, defined by the glide polar curve, are crucial for understanding flight performances: (1) "minimum sink" which provides maximum gliding time from a given height (it results in a minimal rate for losing height) and (2) the "best glide" providing maximum horizontal travel distance from a given height. The best glide is defined where the glide ratio (ratio between the horizontal and vertical speed) is the highest and can be determined by drawing a tangent from the origin. Figure 2 shows the empirical polar curves for the 12 species, highlighting the minimum sink point (indicated by circles) and the maximum glide ratio point (indicated by triangles) for each species. Note that despite *F. naumanni* and *C. ciconia* exhibiting a similar

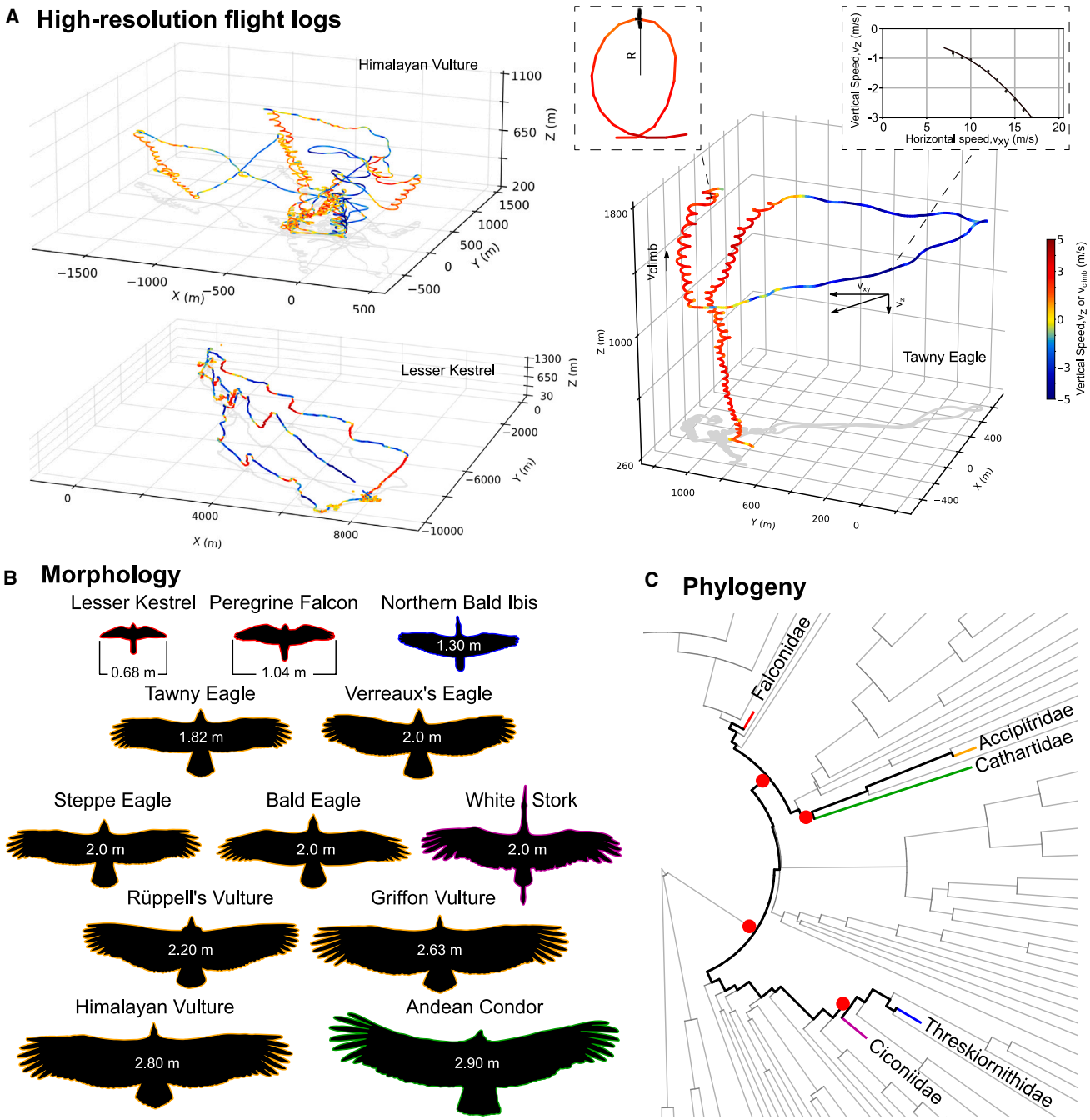


**Figure 1. Overview of our study**

High-frequency GPS datasets of 12 bird species were collected to understand unpowered flight mechanics and behavior (A) and their connections to morphological traits (B), and phylogenetic relatedness (C).

(A) Example trajectories for three individuals from different species. Color-coding indicates vertical speed: positive values from yellow to red for climbing, and negative values from yellow to blue for sinking.

(B) Visualization of the wing shapes of all species in our study showcasing a large variation in wingspan (depicted on the pictures). Outline colors indicate the taxonomic group the species belongs to (shown on C).

(C) Phylogenetic tree of bird species (Tobias et al.[34]) marked with different colors representing the families of the study species. Red circles show the last common ancestors of different families. The phylogenetic trees were used to explicitly accommodate the phylogenetic non-independence among related taxa (see also Tables S1 and S2).

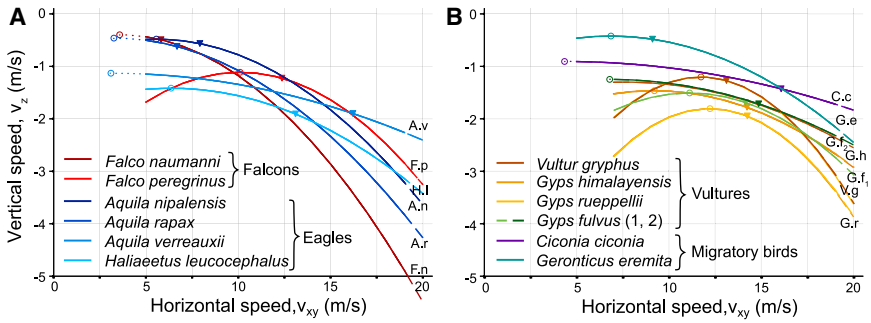


**Figure 2. Empirical polar curves fitted to the flight data presenting the most important features of the gliding**

The relationship between gliding airspeed and vertical speed for 12 species pooled into groups according to genetic relatedness and size similarity: falcons and eagles (A), and vultures and other species (B). Circles denote the minimum sink (the highest point of the parabola fitted to the entire data range). Triangles denote the "best glide" using which birds can travel the furthest from a given height. Dotted and dashed lines indicate the extrapolation of the parabola beyond the range of the used data. (See also Figures S1, S2, and S4; Table S3.).

best glide ratio (also see Table S4 Gliding), they flew at different airspeeds to achieve the best glide.

These flight parameters allowed us to investigate the effects of morphology on flight performance. Wing loading is expected to have a crucial role both in terms of soaring and gliding efficiencies. We studied in detail the functional relationship between wing loading and glide polar characteristics (Figure 3) as previous theoretical and empirical studies of aerodynamics for birds[12,50] and aircrafts[14,51] suggest relationships (see supplemental information Text for details). We found a positive relationship between wing loading and horizontal speed both for best glide ratio (phylogenetic generalized least squares [PGLS] regressions, with coefficient of determination $R^2 = 0.36$, $n = 12$, $p < 0.0001$, $\lambda < 0.0001$, where $\lambda$ is phylogenetic signal estimated by the PGLS model) and for minimum sink speed ($R^2 = 0.25$, $n = 12$, $p < 0.0001$, $\lambda < 0.0001$; Figure 3B). Furthermore, during the soaring phase, individuals with higher wing loading typically flew faster and consequently turned with a larger radius, compared to "lighter" species. We assumed that bank angle ($\varnothing$; Pennycuick[12] pp. 266) and air density ($\rho$; Figure S5) were constant and equal to all birds. The relationships between circling radius and other flight parameters, such as wing loading ($R^2 = 0.32$, $n = 12$, $p < 0.0001$, $\lambda < 0.0001$; Figure 3C), or the average horizontal speed ($R^2 = 0.70$, $n = 12$, $p < 0.0001$, $\lambda < 0.0001$; Figure 3D) were previously reported,[12,52] but here we confirm this for a much larger number of species. Besides wing loading, aspect ratio was also expected to affect flight performance during gliding,[16,17] but in our set of species, the differences in aspect ratio (6.27–8.46) were relatively small (as compared to, for example, the variation in wing loading, 2.1–9.1 kg/m$^2$), thus not providing a large enough range to study its effect (Figure S3).

## Cross-country optimization strategy

When birds fly long distances (sometimes referred to as cross-country flight), they rely on multiple thermals and glide between them. Birds may have strategies where thermalling and gliding flight are "linked" to achieve a specific optimized goal. For example, these strategies could maximize the overall distance traveled for a given period, which takes into account the strengths of the thermals and aerodynamic constraints that shape the glide polar curve. To investigate cross-country optimization strategies between species, we explored how inter-thermal horizontal speed depends upon thermal strength. We used a linear approximation $v_{xy} = A\, v_{climb}^{Thermal} + B$ to represent the relationship between horizontal speed during inter-thermal flight, $v_{xy}$, and climb speed, $v_{climb}^{Thermal}$. The slope of the fitted line ($A$) represents *thermal-strength adaptivity*, i.e., how much the inter-thermal horizontal speed depends on thermal strength (Figure 4A). The intercept ($B$) captures the *preferred inter-thermal gliding speed in zero thermal conditions*.

We calculated the thermal-strength adaptivity ($A_{\text{Observed}}$) by fitting the model to the observed flight data to evaluate the different species' behavior and compare it to the optimum based on MacCready theory ($A_{\text{MacCready}}$). Importantly, while $A_{\text{Observed}}$ only depended on the observed data without explicit assumptions about their polar curve, $A_{\text{MacCready}}$ could only be calculated with the assumption that this polar curve was known. Here, we used our estimated empirical polar curves to estimate the speeds suggested by the MacCready formula.

Based on this comparison, we found that the behavior of the species could be roughly divided into three different categories: (1) $A_{\text{Observed}} > 0$ and $A_{\text{Observed}} \sim A_{\text{MacCready}}$, (2) $A_{\text{Observed}} > 0$ and $A_{\text{Observed}} < A_{\text{MacCready}}$, and (3) $A_{\text{Observed}} \sim 0$ (See Figures 4B–4D), where we mean $A_{\text{Observed}} > 0$ when it is significantly larger than 0 as compared to the randomization test and $A_{\text{Observed}} \sim 0$ otherwise (Tables 1 and S5, see more details in the following text).

We found large variations in $A_{\text{Observed}}$ across species, meaning that species adopt different strategies when choosing their inter-thermal horizontal speed as a function of the strength of the thermals. Six species (*F. naumanni*, *F. peregrinus*, *A. rapax*, *A. nipalensis*, *G. himalayensis*, and adult *G. fulvus)* fall within group 1, as their $A_{\text{Observed}}$ was relatively high (i.e., significantly larger than 0 compared by randomization test, Table S5). This means their gliding speeds depended strongly on thermal strength. In addition, their cross-country optimization reached close to the full potential suggested by the MacCready theory, as shown by their $A_{\text{Observed}}$ close to $A_{\text{MacCready}}$ (Figure 4A, taking into account the accuracy of the parameter estimation). *F. naumanni* applied the highest degree of optimization among the species ($A_{\text{Observed}} = 4.5$). *A. rapax* had the second highest slope ($A_{\text{Observed}} = 3.2$). Except for both eagles (*A. rapax* and *A. nipalensis*), species chose similar, although somewhat lower, *B* values to the MacCready optimum (Figure 4C), which means taking a bit slower horizontal speed between thermals.

Vultures also seemed to be able to adjust their flight speed according to their daily climb speed, and the optimization tendency of *G. himalayensis* ($A_{\text{Observed}} = 1.89$, $p = 0.002$, Table

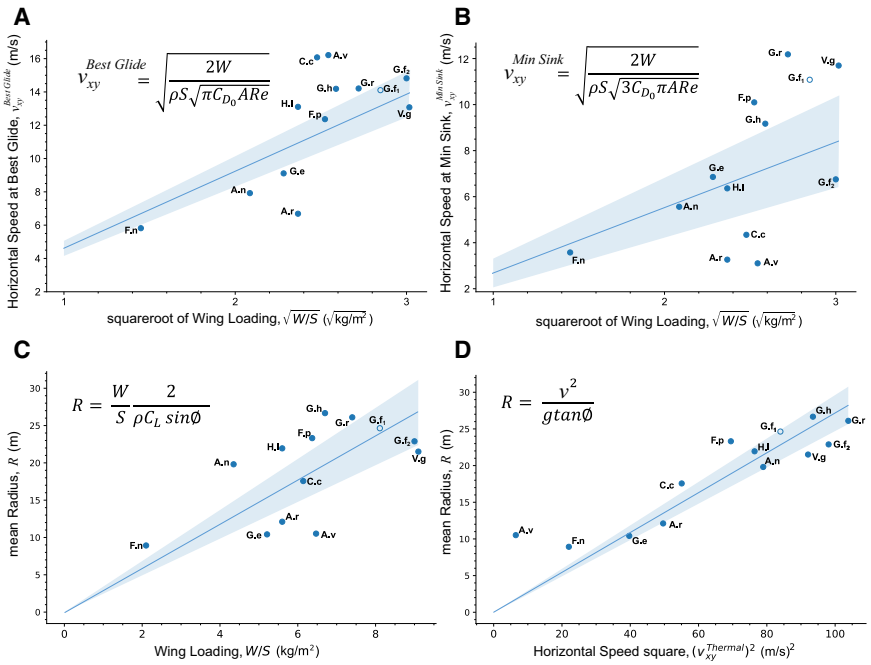


**Figure 3. Relationship between flight behavior and morphological parameter, and comparison to theoretical predictions**

Circles present the mean values for species (with a two-letter abbreviation using the Latin name; see Table S1). Line shows the no-intercept linear fit to the data points accounting for phylogenetic relatedness between the species using a phylogenetic generalized linear model (PGLM). Confidence bands (slopes with plus and minus two standard deviation) are indicated as the shaded areas. As for PGLM only one data point is allowed for a species, in case of the two datasets from *Gyps fulvus*, the larger dataset is used (dataset 2), and the other was discarded (dataset 1; indicated with an open circle). The formula presented on each plot was derived from aerodynamic theory of unpowered flight.

(A and B) Wing loading (*W*/*S*) determines the speed at maximum glide ratio (A, $R^2 = 0.36$, $n = 12$, $p < 0.0001$, $\lambda < 0.0001$) and minimum sink rate (vertical speed) (B, $R^2 = 0.25$, $n = 12$, $p < 0.0001$, $\lambda < 0.0001$), but wing aspect ratio (*AR*), zero-lift drag coefficient ($C_{D0}$), air density ($\rho$), and Oswald efficiency factor (*e*) also have an effect.

(C and D) Scatterplots show the relationship between the radius of the turn in steady flight and wing loading (*W*/*S*, on C, $R^2 = 0.32$, $n = 12$, $p < 0.0001$, $\lambda < 0.0001$) or the horizontal speed ($v_{xy}$) in the thermal (D, $R^2 = 0.70$, $n = 12$, $p < 0.0001$, $\lambda < 0.0001$). A perfect linear relationship would only be expected if all other factors, such as $\rho$, the lift coefficient ($C_L$), and the bank angle (∅) are held constant and are equal for all birds (see more about this assumption in the study by Williams H.J. et al.[53], and for additional information see Figure S4). (See also Figure S3; Tables S2, S4, and S6.).

S5) was similar to adult *G. fulvus* of dataset 1 ($A_{Observed} = 2.32$, $p < 0.001$, Table S5) but not for the mixed-aged birds of dataset 2.

In contrast, two species (*A. verreauxii* and the mixed-aged dataset of *G. fulvus)* can be categorized as group 2 where birds apply a thermal strength adaptive strategy ($A_{Observed} > 0$) when choosing their inter-thermal speed, but the level of adaptivity is considerably smaller than suggested by the MacCready theory ($A_{Observed} < A_{MacCready}$). We analyzed the two *G. fulvus* datasets separately (Figure S4), and found that the thermal strength adaptivity was much higher for dataset 1 ($A^{(1)}_{Observed} > A^{(2)}_{Observed}$). Thus, birds of dataset 2 used suboptimal speeds compared to MacCready while birds of dataset 1 used it close to optimal ($A^{(1)}_{Observed} \sim A^{(1)}_{MacCready}$). We investigated the differences in detail later. For *A. verreauxii* respective $B_{Observed}$ values were also much smaller as compared to the optimal ($B_{Observed} < B_{MacCready}$).

The third group contained only a single species from our datasets, C. *ciconia*. They did not apply an adaptive strategy for choosing their cross-country speed based on thermal strength, as their $A_{Observed}$ was close to zero. The data came from multiple individuals that fly as a flock, so this could be an effect of a collective decision on the flight speed selection.[54]

Finally, we explored whether there is a general relationship between the parameters $A_{Observed}$ and $B_{Observed}$ across the species to understand which thermal-strength dependent strategy birds use. The adaptivity ($A_{Observed}$) was strongly correlated to the preferred no-thermal gliding speed ($B_{Observed}$), meaning that the observed cross-country strategy birds apply has only one free parameter (instead of two; negative correlation, $R^2 = 0.86$, $n = 8$, $p = 0.001$, $\lambda < 0.0001$, Figure 5B). This was also the case when examining individual griffon vultures (determination coefficient, $R^2 = 0.83$, $n = 10$, $F(1,8) = 38.59$, $p = 0.0002$, Figure 5C). Birds with lower inter-thermal gliding speed in zero thermal conditions ($B_{Observed}$) were using a highly adaptive strategy (high values of $A_{Observed}$), and vice versa. Also, we found a strong correlation between $B_{Observed}$ and the horizontal speed at best glide ($R^2 = 0.71$, $n = 8$, $p = 0.086$, $\lambda < 0.0001$, Figure 5A). Thus, birds seem to optimize their flight speed by typically using the "best glide" when thermals are weak. Overall, the linear trend found between $A_{Observed}$ and $B_{Observed}$ (Figure 5B) defined a relationship that was general throughout all studied species (and individuals within species, Figure 5C), so represents a characterization of the cross-country strategy (Figure 5D for the idealistic linear relationship, then for real data on Figures 5E and 5F).

## DISCUSSION

A comprehensive tracking dataset of birds freely flying has enabled us to quantify how morphology and thermal conditions affect flight performance and behavior in different soaring species. The growing literature studying flight behavior of soaring birds by using high-frequency GPS data[55–59] allowed us to do a systematic comparison, to assess previous theoretical predictions and to discover a general rule describing cross-country optimization.

During flight, soaring birds exploit ascending currents to travel large distances without or only a reduced amount of flapping flight. Our results confirmed the aerodynamic theory, as we show relationships between the wing loading and horizontal speed at crucial points of the polar curve (i.e., maximum glide

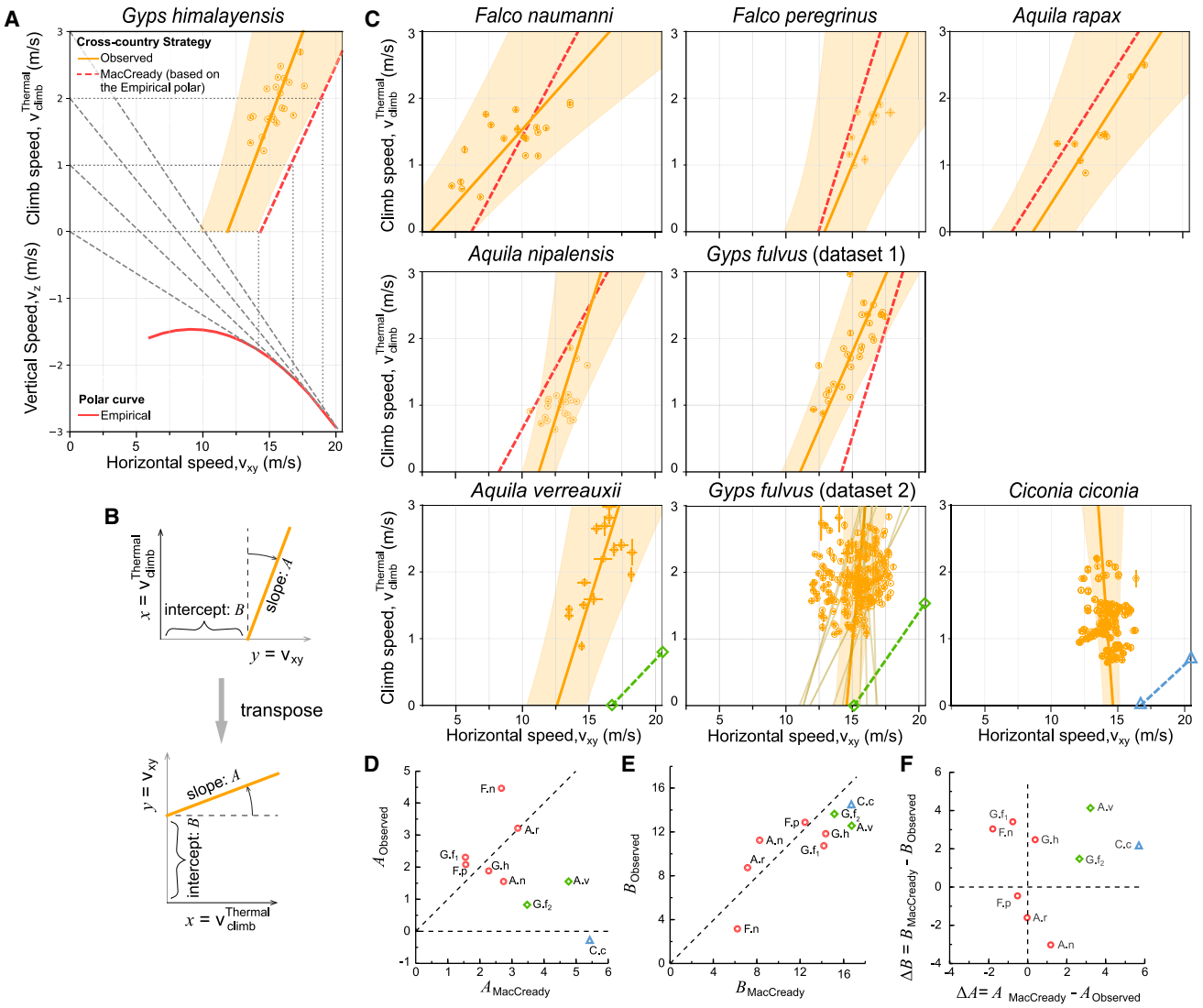


**Figure 4. Evaluating cross-country optimization strategies for different species**

(A) Large plot at top-left provides full overview of the analysis using data of *G. himalayensis*. Solid (red) line shows empirical polar curve at bottom half. Dashed (red) line at top half represents the optimal soaring strategy using MacCready theory. Orange circles show daily individual means with error bars indicating the standard error of the mean, the orange lines were fitted to the data, shaded areas depict confidence bands. We used a linear approximation of the optimal soaring curve, for easier comparison to the real data. Note that the climb speed (y axis) is the independent variable used on the linear fit (slope *A* represents *thermal-strength adaptivity*, and intercept (*B*) captures the *preferred inter-thermal gliding speed in zero thermal conditions*).

(B) Schematic illustration of the linear fitting method. In (A) and (C) we chose an intuitive layout where $v_{climb}$ which encodes vertical motion shown on the vertical axis (y), and $v_{xy}$ which encodes horizontal motion shown on the horizontal axis (x). However, $v_{climb}$ is the independent variable (typically presented on the x axis) and to obtain the intercept and slope of this relationship, we transposed this relationship. Thus, a vertical line on (C) corresponds to a line with 0 slope.

(C) Relationships between climb speed and inter-thermal horizontal speed for all species with at least 10 different flight days (see STAR Methods and panel A). Empirical polar curves are not shown. The colors indicate the three observed cross-country optimization strategies: red - thermal strength-dependent strategy according to MacCready, green line and diamond marker - thermal strength-dependent optimization sub-optimal to MacCready, blue (triangle) - choosing gliding speed independent of thermal strength.

(D and E) Scatterplots showing A (and B) values for the species from the line fitted to flight data ($A_{Observed}$ and $B_{Observed}$, respectively) versus the value ($A_{MacCready}$ and $B_{MacCready}$, respectively) of optimal gliding strategy as calculated using the MacCready theory from the empirical polar fitted to the gliding data.

(F) Scatterplot indicating differences between the observed and the MacCready suggested parameters for *A* and *B*. (See also Figures S4 and S5.).

ratio and minimum sink speed). Furthermore, we found that species whose wing loading was higher typically flew faster, and consequently turned on a larger radius, than lighter ones (Figure 3C). The combination of circling radius and minimum sink speed determines the maximum benefits soaring birds can obtain from thermals. Since both flight aspects primarily depend on wing loading, species with lower wing loading outperform those with higher wing loading in the same thermal.

**Table 1. Metrics of gliding flight and thermal-strength adaptivity**

| Species | Best glide ratio 1 | $v_{xy}$ at best glide m/s | $v_{xy}$ at min sink m/s | $v_z$ at min sink m/s | $A_{Observed}$ 1 | $B_{Observed}$ m/s |
|---|---|---|---|---|---|---|
| *Falco naumanni* | 11.8 | 5.81 | 3.57 | −0.4 | 4.48 | 3.16 |
| *Falco peregrinus* | 10.8 | 12.36 | 10.1 | −1.11 | 2.09 | 12.9 |
| *Haliaeetus leucocephalus* | 6.86 | 13.1 | 6.36 | −1.41 | – | – |
| *Aquila nipalensis* | 14 | 7.92 | 5.56 | −0.48 | 1.56 | 11.27 |
| *Aquila verreauxii* | 8.53 | 16.21 | 3.10 | −1.13 | 1.56 | 12.59 |
| *Aquila rapax* | 10.75 | 6.68 | 3.26 | −0.46 | 3.22 | 8.75 |
| *Gyps fulvus* (dataset 1) | 8.36 | 14.1 | 11.07 | −1.50 | 2.32 | 10.75 |
| *Gyps fulvus* (dataset 2) | 8.64 | 14.81 | 6.75 | −1.24 | 0.83 | 13.65 |
| *Gyps himalayensis* | 7.98 | 14.18 | 9.17 | −1.46 | 1.89 | 11.85 |
| *Gyps rueppellii* | 7.31 | 14.2 | 12.18 | −1.80 | – | – |
| *Vultur gryphus* | 10.31 | 13.07 | 11.7 | −1.20 | – | – |
| *Geronticus eremita* | 18.91 | 9.1 | 6.85 | −0.42 | – | – |
| *Ciconia ciconia* | 11.26 | 16.07 | 4.34 | −0.90 | −0.26 | 14.53 |

Gliding parameters derived from the empirical glide polar and parameters of cross-country optimization strategy where $A_{Observed}$ is *thermal-strength adaptivity*, and $B_{Observed}$ captures the *preferred inter-thermal gliding speed in zero thermal conditions*. $A_{Observed}$ and $B_{Observed}$ are only calculated and presented for 8 species with at least 10 different flight days (see STAR Methods).

These species-specific features and choices contribute to the observed general cross-country trend. We explored how different species adapt their cross-country strategies depending on thermal strength (Figure 4). We found that the preferred no-thermal gliding speed $B_{Observed}$ was close to the maximum glide ratio (that allows the birds to travel the farthest from a given altitude), meaning that birds optimize gliding speed in relation to their aerodynamic properties (Figure 5A). We observed a negative relationship between $A_{Observed}$ and $B_{Observed}$ across all species (and between individuals for a single species). We also show that this thermal strength-dependent optimization strategy was highly related to certain morphological parameters. More specifically, species (individuals) with lower wing loading adopt a strategy where their inter-thermal gliding speed depends more strongly on thermal strength. Lower wing loading allows them to circle closer to the core of the thermal (where it is the strongest) and experience stronger lifts.[53] Also, our results show that the average horizontal speed in the thermals was correlated to the horizontal speed at minimum sink speed ($R^2 = 0.73$), which allows a bird to take advantage of even weak thermals. We found that wing loading was a major deterministic morphological feature that defines the horizontal speed at the minimum sink speed (as seen in Figure 3B).

The combination of these two effects (i.e., the relationships of wing loading to inter-thermal glide speed and minimum sink speed) allows birds with lower wing loading to gain even higher benefits in the thermal, reaching higher climb speeds. On the other hand, these birds can afford to choose their inter-thermal speed more boldly and thus travel at a higher speed in good thermalling conditions. Our thermal-strength adaptivity ($A_{Observed}$) results depend not on the glide polar and the related MacCready speed-to-flight theory[31] but only on horizontal speed selection related to the daily average climb speed. MacCready theory does not take into account other environmental parameters for cross-country flights, such as the number of exploited thermals per day or the distance between thermals. Following MacCready theory causes a risk of being grounded or to avoid that, the need for switching to costly flapping flight for birds.[21] Other environmental factors[60,61] could cause similar risks. For this reason, birds that show a high degree of thermal-strength adaptivity can be considered more risk-prone species. Furthermore, our results confirm the previous findings about *F. peregrinus* and *A. nipalensis* that the relation between flight speed and updraft strength is correlated and follows MacCready theory.[32,33,62]

Variation between bird species in morphological features and flight style was related to the species' behavior and ecological needs.[11,63–67] In general, birds' wing shapes are generally evolved to minimize the energy costs of flying at their typical speed and flight mode[63,68] but they still need to perform other phases of flight, such as take-off and aerial attack, which are related to their species-specific niches. For our species, although all raptors rely heavily on thermals to facilitate low-cost foraging flight, *F. peregrinus* requires more agility to capture aerial prey. In contrast, eagle species employ powerful attacks on prey on the ground and in the air. Similarly, all scavengers need to maximize their flight distance to locate carcasses, and a high capability for manoeuvrability is not necessary, as they do not typically attack moving animals. *C. ciconia* and *G. eremita* predominantly feed on the ground and perform long-range migration. Thus, adapting to these species-specific environments results in variations in the flight performance and behavior of bird species. For this reason, maximizing the flight range might not be the only purpose during the flight. There might be several different optimizations by birds, such as keeping the prey attack range, maximizing the flight duration or migrating as a flock.

Apart from species differences, individual birds may also exhibit variation in flight performance due to differences in lifetime stage (e.g., age, breeding status, and migration strategy). For example, older soaring birds may tolerate larger amounts

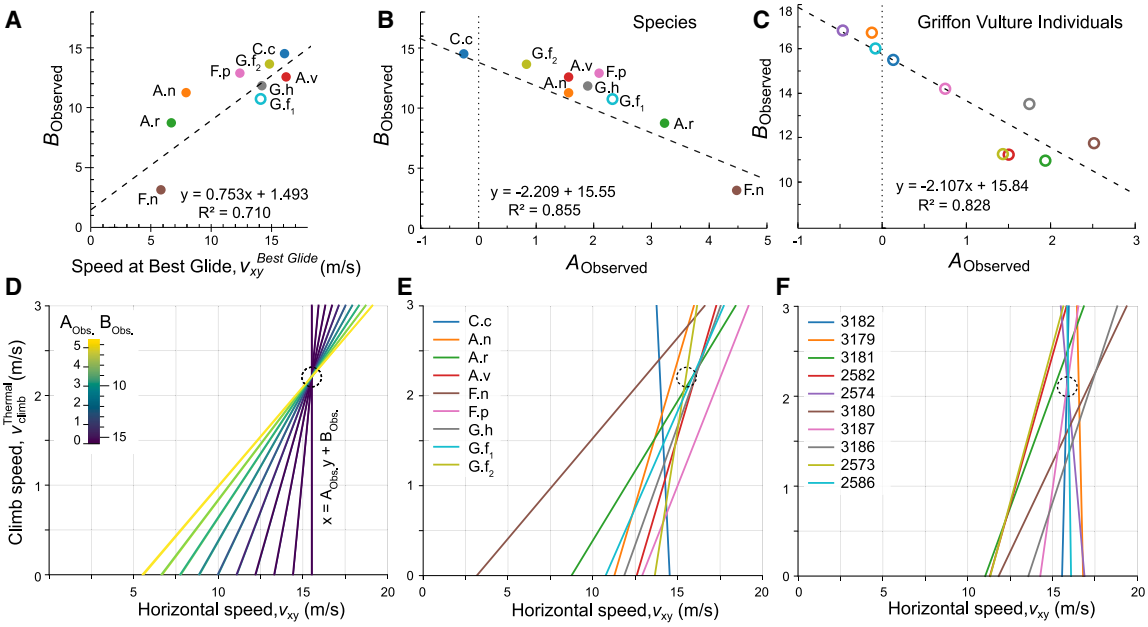


**Figure 5. Relationship between the parameters of cross-country optimization strategy for all species and for individual Griffon vultures**

To characterize cross-country behavior, we fitted for each species a line to the horizontal speed $v_{xy}$ during inter-thermal flight as a function of the climb speed $v_{climb}^{Thermal}$ (that relates to the strength of the thermals) as $v_{xy} = A_{Obs.} v_{climb}^{Thermal} + B_{Obs.}$.

(A) Relationship between $B_{Observed}$ and the horizontal speed at best glide.

(B) Relationship between $B_{Observed}$ and $A_{Observed}$ for all species. Dashed line shows the PGLS linear fit to the data.

(C) As B, just for individual Griffon vultures, as dataset 2 was large enough to analyze the cross-country behavior individually.

(D) The linear relationship between $A_{Obs.}$ and $B_{Obs.}$ (as shown on Figure 5B and 5C) means that the lines defined as $v_{xy} = A_{Obs.} v_{climb}^{Thermal} + B_{Obs.}$ have special characteristics. Here, we show the possible lines on the $v_{climb}^{Thermal}$ and $v_{xy}$ diagram (as in Figure 4A) for different $A_{Obs.}$ and $B_{Obs.}$ values indicated by their color coding, ranging $A_{Obs.} = 0$ (no thermal adaptivity, dark blue) to $A_{Obs.} = 5$ (a highly adaptive strategy, yellow). The relationship between $A_{Obs.}$ and $B_{Obs.}$ means that they are coupled, and thus the lines follow a pattern where each goes through a single point (marked with the dashed circle). The coordinates of this point are determined by the coefficients of the linear fit shown on (B), (x = 15.55, y = 2.209). Note that the inter-thermal horizontal speed, $v_{xy}$ (x axis) is a function of the climb speed, $v_{climb}^{Thermal}$ (y axis).

(E and F) The cross-country strategy lines are shown for each species (on E) and for individual Griffon vultures (F), using the same axes and ranges as on (D). The dashed circles show the point defined by the fitted line on (B) and (C), respectively. The color codes match the respective plots on (B) and (C). (See also Table S5.).

of flapping flight during migration to reach their breeding grounds earlier.[69] Alternatively, birds with different experiences may differ in their skills to exploit thermals or soar under challenging wind conditions.[36] Here, we observed notable inter-individual differences in the strategies of Griffon vultures. Adult Griffon vultures vary in their flight speeds and flight height according to the motivation and flight purpose (migration vs. foraging flight, outbound vs. inbound flight[36]). Thus, experience or developmental stage (e.g., developments of flight muscles) may cause variations in thermal strength adaptivity and the related selection of horizontal speed in the mixed-aged dataset of the Griffon vultures. It has been previously reported that adult vultures demonstrate superior abilities compared to juveniles in utilizing thermals, even though they have similar wing loading.[36] A similar effect probably applies to inter-thermal speed selection, since experienced birds use tailwind more efficiently[36] and may assess the location of the next thermals better. On the other hand, birds that take advantage of the same thermal within a similar period can use visual cues from birds ahead that already discovered the thermal, allowing them to use the thermal core directly.[70,71] This use of social information increases the efficiency of their net altitude gain in thermals, which may directly lead to changes in their strategic choices. Moreover, during long-range cross-country flights, visual cues can help them predict the abundance and locations of thermals, which can significantly influence their strategy.[72] In addition to behavioral differences, morphological traits can vary strongly within species and even within individuals. For example, although wing features show little variation within adults, body mass can fluctuate substantially depending on whether the bird is carrying a meal or not. In summary, although there are various factors at individual- and species-level that can influence the flight performance of soaring birds, our comparative analyses discovered a general, empirical rule that describes the cross-country strategies across all analyzed species.

## Limitations of the study

Although GPS devices have successfully recorded flight tracks, significant challenges remain when it comes to identifying flight styles, for example distinguishing between flapping and non-flapping flight. Specifically, our attempt to classify gliding and soaring is not purely based on fixed-wing flight aerodynamics, as it likely includes flapping flight. Additionally, we collected

morphological data for the species from various sources, which may influence the observed relationships between the flight metrics and morphological traits. Nevertheless, when thinking about future direction in this research field, we believe our study has established a foundation for understanding the cross-country strategies of soaring birds and with it groundwork for technical developments like autonomous soaring drones.

## RESOURCE AVAILABILITY

### Lead contact

Further information and requests for resources and reagents should be directed to and will be fulfilled by the lead contact, Máté Nagy (mate.nagy@ttk.elte.hu).

### Materials availability

This study did not generate new specimens or materials. All images are included in the text and Supporting Information.

### Data and code availability

- All data reported in this paper is available on the repository: Zenodo: https://doi.org/10.5281/zenodo.12607007.
- The code is available on the repository: Github: https://github.com/gokselkeskin/adaptive-soaring-strategy.

## ACKNOWLEDGMENTS

We thank authors who shared their published data, namely Roi Harel, Jesus Hernandez-Pliego, Megan Murgatroyd, Ran Nathan, Kate Reynolds, Graham Taylor, Bernhard Voelkl, and Johannes Fritz. G.K. was supported by Stipendium Hungaricum. This research was partially supported by Eötvös Loránd University and the Hungarian Academy of Sciences (grant number 95152). This project was partially supported by the National Research, Development and Innovation Office under grant no. K128780. M.N. acknowledges support from the Isaac Newton Institute for Mathematical Sciences for support and hospitality during the program "Mathematics of Movement: an interdisciplinary approach to mutual challenges in animal ecology and cell biology", supported by the EPSRC grant number EP/R014604/1. P.L. was supported by Eötvös Loránd University, CollMot Robotics Ltd. and the Ministry of Culture and Innovation of Hungary from the National Research, Development and Innovation Fund (awarded to P.L., project no. C1794246, KDP-2021 funding scheme). O.D. acknowledges the staff of Rocher des Aigles, Rocamadour, France, for long-term support of experiments using captive raptors since 2010: R. Arnaud, D. Maylin, B. Nouzière, and all falconry staff. O.D. also thank C. Tromp, Y. Ropert-Coudert, A. Kato, and several students for data collection between 2010 and 2014. O.D. thanks Giacomo Dell'Omo and the team from TechnoSmart who provided high-frequency GPS tags and accelerometers. A.F. was supported by the Germany Research Foundation (DFG, Emmy Noether Fellowship 463925853), the Max Planck Society, the Hans und Helga Maus-Stiftung, and the James Heinemann research award of the Minerva Stiftung.

## AUTHOR CONTRIBUTIONS

G.K., O.D., and M.N. conceived the idea and designed the project; O.D. collected experimental data; G.K. collected and standardized our original and the previously published datasets; G.K. and M.N. designed the data analysis with contribution from O.D. and A.F; G.K., P.L., and M.N. analyzed the data; G.K., A.F., and M.N. wrote the paper with contributions from O.D. and P.L.; All authors revised the manuscript.

## DECLARATION OF INTERESTS

The authors declare no competing interests.

## STAR★METHODS

Detailed methods are provided in the online version of this paper and include the following:

- KEY RESOURCES TABLE
- EXPERIMENTAL MODEL AND STUDY PARTICIPANT DETAILS
  - Datasets
- METHOD DETAILS
  - Data preparation
  - Evaluation of gliding and thermalling phases of flight
  - Cross-country strategy
  - Generating a theoretical glide polar using the Pennycuick's flight tool
  - Phylogenetic analysis
- QUANTIFICATION AND STATISTICAL ANALYSIS
  - Randomization test

## SUPPLEMENTAL INFORMATION

Supplemental information can be found online at https://doi.org/10.1016/j.isci.2025.112090.

Received: July 23, 2024
Revised: November 22, 2024
Accepted: February 19, 2025
Published: February 22, 2025

## REFERENCES

1. Hedenström, A. (1997). Predicted and observed migration speed in Lesser Spotted Eagle Aquila pomarina. Ardea *85*, 29–35.
2. Shamoun-Baranes, J., Bouten, W., Van Loon, E.E., Meijer, C., and Camphuysen, C.J. (2016). Flap or soar? How a flight generalist responds to its aerial environment. Philos. Trans. R. Soc. Lond. B Biol. Sci. *371*, 20150395. https://doi.org/10.1098/rstb.2015.0395.
3. Lasiewski, R.C., and Dawson, W.R. (1967). A re-examination of the relation between standard metabolic rate and body weight in birds. Condor *69*, 13–23. https://doi.org/10.2307/1366368.
4. Pennycuick, C.J. (1972). Soaring behaviour and performance of some East African birds, observed from a motor-glider. Ibis *114*, 178–218. https://doi.org/10.1111/j.1474-919X.1972.tb02603.x.
5. Askew, G.N., and Ellerby, D.J. (2007). The mechanical power requirements of avian flight. Biol. Lett. *3*, 445–448. https://doi.org/10.1098/rsbl.2007.0182.
6. Taylor, G.K., and Thomas, A.L.R. (2014). Evolutionary Biomechanics: Selection, Phylogeny, and Constraint (Oxford University Press).
7. Mueller, H.C. (1991). Flight Strategies of Migrating Hawks. Wilson Bull. *103*, 331–333. https://doi.org/10.1126/science.248.4961.1429.
8. Spaar, R., and Bruderer, B. (1996). Soaring migration of Steppe Eagles Aquila nipalensis in southern Israel: flight behaviour under various wind and thermal conditions. J. Avian Biol. *27*, 289–301. https://doi.org/10.2307/3677260.
9. Pennycuick, C.J. (1998). Field observations of thermals and thermal streets, and the theory of cross-country soaring flight. J. Avian Biol. *29*, 33–43. https://doi.org/10.2307/3677338.
10. Pennycuick, C.J. (2003). The concept of energy height in animal locomotion: separating mechanics from physiology. J. Theor. Biol. *224*, 189–203. https://doi.org/10.1016/S0022-5193(03)00157-7.
11. Norberg, U.M. (1990). Vertebrate Flight (Oxford University Press). https://doi.org/10.1002/j.2326-1951.1962.tb00477.x.
12. Pennycuick, C.J. (2008). Modelling the Flying Bird (Elsevier).
13. Norberg, U.M., and Rayner, J.M.V. (1987). Ecological morphology and flight in bats (Mammalia; Chiroptera): wing adaptations, flight

performance, foraging strategy and echolocation. Philos. Trans. R. Soc. Lond. B Biol. Sci. *316*, 335–427. https://doi.org/10.1098/rstb.1987.0030.

14. Thomas, F., and Milgram, J. (1999). Fundamentals of Sailplane Design (College Park Press).
15. Vogel, S. (2013). Comparative Biomechanics: Life's Physical World (Princeton University Press).
16. Waldrop, L.D., He, Y., Hedrick, T.L., and Rader, J.A. (2020). Functional morphology of gliding flight I: modeling reveals distinct performance landscapes based on soaring strategies. Integr. Comp. Biol. *60*, 1283–1296. https://doi.org/10.1093/icb/icaa114.
17. Rader, J.A., Hedrick, T.L., He, Y., and Waldrop, L.D. (2020). Functional morphology of gliding flight II. Morphology follows predictions of gliding performance. Integr. Comp. Biol. *60*, 1297–1308. https://doi.org/10.1093/icb/icaa126.
18. Shamoun-Baranes, J., Leshem, Y., Yom-Tov, Y., and Liechti, O. (2003). Differential use of thermal convection by soaring birds over central Israel. Condor *105*, 208–218. https://www.jstor.org/stable/1370541.
19. Leshem, Y., and Yom-Tov, Y. (1996). The use of thermals by soaring migrants. Ibis *138*, 667–674. https://doi.org/10.1111/j.1474-919X.1996.tb04768.x.
20. Spaar, R. (1997). Flight strategies of migrating raptors; a comparative study of interspecific variation in flight characteristics. Ibis *139*, 523–535. https://doi.org/10.1111/j.1474-919X.1997.tb04669.x.
21. Horvitz, N., Sapir, N., Liechti, F., Avissar, R., Mahrer, I., and Nathan, R. (2014). The gliding speed of migrating birds: Slow and safe or fast and risky? Ecol. Lett. *17*, 670–679. https://doi.org/10.1111/ele.12268.
22. Shelton, R.M., Jackson, B.E., and Hedrick, T.L. (2014). The mechanics and behavior of cliff swallows during tandem flights. J. Exp. Biol. *217*, 2717–2725. https://doi.org/10.1242/jeb.101329.
23. Evangelista, D.J., Ray, D.D., Raja, S.K., and Hedrick, T.L. (2017). Three-dimensional trajectories and network analyses of group behaviour within chimney swift flocks during approaches to the roost. Proc. Biol. Sci. *284*, 20162602. https://doi.org/10.1098/rspb.2016.2602.
24. Hedrick, T.L., Pichot, C., and de Margerie, E. (2018). Gliding for a free lunch: biomechanics of foraging flight in common swifts (Apus apus). J. Exp. Biol. *221*, jeb186270. https://doi.org/10.1242/jeb.186270.
25. Shannon, H.D., Young, G.S., Yates, M.A., Fuller, M.R., and Seegar, W.S. (2002). American white pelican soaring flight times and altitudes relative to changes in thermal depth and intensity. Condor *104*, 679–683. https://www.jstor.org/stable/1370751.
26. Weimerskirch, H., Le Corre, M., Ropert-Coudert, Y., Kato, A., and Marsac, F. (2005). The three-dimensional flight of red-footed boobies: adaptations to foraging in a tropical environment? Proc. Biol. Sci. *272*, 53–61. https://doi.org/10.1098/rspb.2004.2918.
27. Voelkl, B., and Fritz, J. (2017). Relation between travel strategy and social organization of migrating birds with special consideration of formation flight in the northern bald ibis. Phil. Trans. R. Soc. B *372*, 20160235. https://doi.org/10.1098/rstb.2016.0235.
28. Hernández-Pliego, J., Rodríguez, C., Dell'Omo, G., and Bustamante, J. (2017). Combined use of tri-Axial accelerometers and GPS reveals the flexible foraging strategy of a bird in relation to weather conditions. PLoS One *12*, 1–29. https://doi.org/10.1371/journal.pone.0177892.
29. Murgatroyd, M., Photopoulou, T., Underhill, L.G., Bouten, W., and Amar, A. (2018). Where eagles soar: Fine-resolution tracking reveals the spatio-temporal use of differential soaring modes in a large raptor. Ecol. Evol. *8*, 6788–6799. https://doi.org/10.1002/ece3.4189.
30. Baliga, V.B., Szabo, I., and Altshuler, D.L. (2019). Range of motion in the avian wing is strongly associated with flight behavior and body mass. Sci. Adv. *5*, eaaw6670. https://doi.org/10.1126/sciadv.aaw6670.
31. MacCready, P.B. (1958). Optimum airspeed selector. Soaring *11*, 10.
32. Akos, Z., Nagy, M., and Vicsek, T. (2008). Comparing bird and human soaring strategies. Proc. Natl. Acad. Sci. USA *105*, 4139–4143. https://doi.org/10.1073/pnas.0707711105.
33. Taylor, G.K., Reynolds, K.V., and Thomas, A.L.R. (2016). Soaring energetics and glide performance in a moving atmosphere. Philos. Trans. R. Soc. Lond. B Biol. Sci. *371*, 20150398. https://doi.org/10.1098/rstb.2015.0398.
34. Tobias, J.A., Sheard, C., Pigot, A.L., Devenish, A.J.M., Yang, J., Sayol, F., Neate-Clegg, M.H.C., Alioravainen, N., Weeks, T.L., Barber, R.A., et al. (2022). AVONET: morphological, ecological and geographical data for all birds. Ecol. Lett. *25*, 581–597. https://doi.org/10.1111/ele.13898.
35. Duriez, O., Kato, A., Tromp, C., Dell'Omo, G., Vyssotski, A.L., Sarrazin, F., and Ropert-Coudert, Y. (2014). How cheap is soaring flight in raptors? A preliminary investigation in freely-flying vultures. PLoS One *9*, e84887. https://doi.org/10.1371/journal.pone.0084887.
36. Harel, R., Horvitz, N., and Nathan, R. (2016). Adult vultures outperform juveniles in challenging thermal soaring conditions. Sci. Rep. *6*, 27865. https://doi.org/10.1038/srep27865.
37. Masden, E.A., Haydon, D.T., Fox, A.D., Furness, R.W., Bullman, R., and Desholm, M. (2009). Barriers to movement: impacts of wind farms on migrating birds. ICES J. Mar. Sci. *66*, 746–753. https://doi.org/10.1093/icesjms/fsp031.
38. Baisner, A.J., Andersen, J.L., Findsen, A., Yde Granath, S.W., Madsen, K.Ø., and Desholm, M. (2010). Minimizing collision risk between migrating raptors and marine wind farms: development of a spatial planning tool. Environ. Manag. *46*, 801–808. https://doi.org/10.1007/s00267-010-9541-z.
39. Alves, J.A., Gunnarsson, T.G., Potts, P.M., Gélinaud, G., Sutherland, W.J., and Gill, J.A. (2012). Overtaking on migration: does longer distance migration always incur a penalty? Oikos *121*, 464–470. http://www.jstor.org/stable/41428991.
40. Cabrera-Cruz, S.A., Mabee, T.J., and Patraca, R.V. (2013). Using Theoretical Flight Speeds to Discriminate Birds from Insects in Radar Studies: Usando Velocidades de Vuelo Teóricas Para Discriminar Aves de Insectos en Estudios de Radar. Condor *115*, 263–272. https://doi.org/10.1525/cond.2013.110181.
41. Šuba, J. (2014). Migrating Nathusius's pipistrelles Pipistrellus nathusii (Chiroptera: Vespertilionidae) optimise flight speed and maintain acoustic contact with the ground. Environ. Exp. Biol. *12*, 7–14.
42. Ksepka, D.T. (2014). Flight performance of the largest volant bird. Proc. Natl. Acad. Sci. USA *111*, 10624–10629. https://doi.org/10.1073/pnas.1320297111.
43. Scullion, F.T., and Scullion, F. (2018). Profiling Flight Performance of Young Racing Pigeons (Columba livia) in Training. J. Vet. Healthc. *1*, 1–19. https://doi.org/10.14302/issn.2575-1212.jvhc-17-1796.
44. Cano, N., Bayly, N.J., and Wilson, S. (2020). Is there more than one way to cross the Caribbean Sea? Migratory strategies of Nearctic-Neotropical landbirds departing from northern Colombia. J. Avian Biol. *51*, 02394. https://doi.org/10.1111/jav.02394.
45. Cannell, A.E. (2020). Too big to fly? An engineering evaluation of the fossil biology of the giant birds of the Miocene in relation to their flight limitations, constraining the minimum air pressure at about 1.3 bar. Anim. Biol. *70*, 251–270. https://doi.org/10.1163/15707563-bja10001.
46. Naish, D., Witton, M.P., and Martin-Silverstone, E. (2021). Powered flight in hatchling pterosaurs: evidence from wing form and bone strength. Sci. Rep. *11*, 13130. https://doi.org/10.1038/s41598-021-92499-z.
47. Rogalla, S., Nicolaï, M.P.J., Porchetta, S., Glabeke, G., Battistella, C., D'Alba, L., Gianneschi, N.C., van Beeck, J., and Shawkey, M.D. (2021). The evolution of darker wings in seabirds in relation to temperature-dependent flight efficiency. J. R. Soc. Interface *18*, 20210236. https://doi.org/10.1098/rsif.2021.0236.
48. Lentink, D., Müller, U.K., Stamhuis, E.J., De Kat, R., Van Gestel, W., Veldhuis, L.L.M., Henningsson, P., Hedenström, A., Videler, J.J., and Van Leeuwen, J.L. (2007). How swifts control their glide performance with morphing wings. Nature *446*, 1082–1085. https://doi.org/10.1038/nature05733.

49. Henningsson, P., and Hedenström, A. (2011). Aerodynamics of gliding flight in common swifts. J. Exp. Biol. *214*, 382–393. https://doi.org/10.1242/jeb.050609.
50. Norberg, U.M. (1990). Vertebrate Flight. Mechanics, Physiology, Morphology, Ecology and Evolution, Zoophysiology. Springer Berlin *27*, 65–75, Gliding flight. https://doi.org/10.1007/978-3-642-83848-4.
51. Anderson, J.D. (1999). Aircraft Performance and Design (WCB/McGraw-Hill).
52. Ákos, Z., Nagy, M., Leven, S., and Vicsek, T. (2010). Thermal soaring flight of birds and unmanned aerial vehicles. Bioinspiration Biomimetics *5*, 045003. https://doi.org/10.1088/1748-3182/5/4/045003.
53. Williams, H.J., Duriez, O., Holton, M.D., Dell'Omo, G., Wilson, R.P., and Shepard, E.L.C. (2018). Vultures respond to challenges of near-ground thermal soaring by varying bank angle. J. Exp. Biol. *221*, jeb174995. https://doi.org/10.1242/jeb.174995.
54. Flack, A., Nagy, M., Fiedler, W., Couzin, I.D., and Wikelski, M. (2018). From local collective behavior to global migratory patterns in white storks. Science *360*, 911–914. https://doi.org/10.1126/science.aap7781.
55. Shepard, E.L.C., Lambertucci, S.A., Vallmitjana, D., and Wilson, R.P. (2011). Energy beyond food: foraging theory informs time spent in thermals by a large soaring bird. PLoS One *6*, e27375. https://doi.org/10.1371/journal.pone.0027375.
56. Bohrer, G., Brandes, D., Mandel, J.T., Bildstein, K.L., Miller, T.A., Lanzone, M., Katzner, T., Maisonneuve, C., and Tremblay, J.A. (2012). Estimating updraft velocity components over large spatial scales: contrasting migration strategies of golden eagles and turkey vultures. Ecol. Lett. *15*, 96–103. https://doi.org/10.1111/j.1461-0248.2011.01713.x.
57. Reynolds, K.V., Thomas, A.L.R., and Taylor, G.K. (2014). Wing tucks are a response to atmospheric turbulence in the soaring flight of the steppe eagle Aquila nipalensis. J. R. Soc. Interface *11*, 20140645. https://doi.org/10.1098/rsif.2014.0645.
58. Hernández-Pliego, J., Rodríguez, C., and Bustamante, J. (2015). Why Do Kestrels Soar? PLoS One *10*, 0145402. https://doi.org/10.1371/journal.pone.0145402.
59. Longarini, A., Duriez, O., Shepard, E., Safi, K., Wikelski, M., and Scacco, M. (2023). Effect of harness design for tag attachment on the flight performance of five soaring species. Mov. Ecol. *11*, 39. https://doi.org/10.1186/s40462-023-00408-y.
60. Shepard, E.L.C., Williamson, C., and Windsor, S.P. (2016). Fine-scale flight strategies of gulls in urban airflows indicate risk and reward in city living. Philos. Trans. R. Soc. Lond. B Biol. Sci. *371*, 20150394. https://doi.org/10.1098/rstb.2015.0394.
61. Richardson, P.L., Wakefield, E.D., and Phillips, R.A. (2018). Flight speed and performance of the wandering albatross with respect to wind. Mov. Ecol. *6*, 3–15. https://doi.org/10.1186/s40462-018-0121-9.
62. Reynolds, K. (2015). Soaring and Gust Response in the Steppe Eagle (University of Oxford).
63. Gill, F.B., and Prum, R.O. (2019). Ornithology (Macmillan).
64. Savile, O.B.O. (1957). Adaptive evolution in the avian wing. Evolution *11*, 212–224. https://doi.org/10.1111/j.1558-5646.1957.tb02889.x.
65. Wang, X., and Clarke, J.A. (2015). The evolution of avian wing shape and previously unrecognized trends in covert feathering. Proc. Biol. Sci. *282*, 20151935. https://doi.org/10.1098/rspb.2015.1935.
66. Jenni-Eiermann, S., and Srygley, R. B. (2018). Physiological aeroecology: anatomical and physiological adaptations for flight. *Aeroecology*. Cham, Springer International Publishing, 87–118. https://doi.org/10.1007/978-3-319-57024-2.
67. Baumgart, S.L., Sereno, P.C., and Westneat, M.W. (2021). Wing shape in waterbirds: morphometric patterns associated with behavior, habitat, migration, and phylogenetic convergence. Integr. Org. Biol. *3*, obab011. https://doi.org/10.1093/iob/obab011.
68. Santos, C.D., Hanssen, F., Muñoz, A.-R., Onrubia, A., Wikelski, M., May, R., and Silva, J.P. (2017). Match between soaring modes of black kites and the fine-scale distribution of updrafts. Sci. Rep. *7*, 6421. https://doi.org/10.1038/s41598-017-05319-8.
69. Aikens, E.O., Nourani, E., Fiedler, W., Wikelski, M., and Flack, A. (2024). Learning shapes the development of migratory behavior. Proc. Natl. Acad. Sci. USA *121*, e2306389121. https://doi.org/10.1073/pnas.2306389121.
70. Nagy, M., Couzin, I.D., Fiedler, W., Wikelski, M., and Flack, A. (2018). Synchronization, coordination and collective sensing during thermalling flight of freely migrating white storks. Philos. Trans. R. Soc. Lond. B Biol. Sci. *373*, 20170011. https://doi.org/10.1098/rstb.2017.0011.
71. Williams, H.J., King, A.J., Duriez, O., Börger, L., and Shepard, E.L.C. (2018). Social eavesdropping allows for a more risky gliding strategy by thermal-soaring birds. J. R. Soc. Interface *15*, 20180578. https://doi.org/10.1098/rsif.2018.0578.
72. Sassi, Y., Nouzières, B., Scacco, M., Tremblay, Y., Duriez, O., and Robira, B. (2024). The use of social information in vulture flight decisions. Proc. R. Soc. B Biol. Sci. *291*, 1729. https://doi.org/10.1098/rspb.2023.1729.
73. Weinzierl, R., Bohrer, G., Kranstauber, B., Fiedler, W., Wikelski, M., and Flack, A. (2016). Wind estimation based on thermal soaring of birds. Ecol. Evol. *6*, 8706–8718. https://doi.org/10.1002/ece3.2585.
74. Flack, A., Fiedler, W., and Wikelski, M. (2017). Data from: Wind estimation based on thermal soaring of birds.
75. Maybury, W.J. (2000). *The Aerodynamics of Bird Bodies*. PhD thesis (University of Bristol).
76. Ortal, H. (2012). *Turbulent Flow Characterization and Aerodynamic Forces Around a Gliding Osprey Model in a Wind Tunnel*. PhD thesis (Ben-Gurion University of the Negev).
77. Pagel, M. (1999). Inferring the historical patterns of biological evolution. Nature *401*, 877–884. https://doi.org/10.1038/44766.
78. Revell, L.J. (2010). Phylogenetic signal and linear regression on species data. Methods Ecol. Evol. *1*, 319–329. https://doi.org/10.1111/j.2041-210X.2010.00044.x.
79. Jetz, W., Thomas, G.H., Joy, J.B., Hartmann, K., and Mooers, A.O. (2012). The global diversity of birds in space and time. Nature *491*, 444–448. https://doi.org/10.1038/nature11631.
80. Revell, L.J. (2024). phytools 2.0: an updated R ecosystem for phylogenetic comparative methods (and other things). PeerJ *12*, e16505. https://doi.org/10.7717/peerj.16505.
81. Grafen, A. (1989). The phylogenetic regression. Phil. Trans. Roy. Soc. Lond. *326*, 119–157. https://doi.org/10.1098/rstb.1989.0106.
82. Paradis, E., and Schliep, K. (2019). ape 5.0: an environment for modern phylogenetics and evolutionary analyses in R. Bioinformatics *35*, 526–528. https://doi.org/10.1093/bioinformatics/bty633.
83. R Development Core Team (2022). R: A Language and Environment for Statistical Computing (R Foundation for Statistical Computing).
84. Dubitzky, W., Wolkenhauer, O., Cho, K.-H., and Yokota, H. (2013). Encyclopedia of Systems Biology (New York, NY, USA: Springer).

# STAR★METHODS

## KEY RESOURCES TABLE

| REAGENT or RESOURCE | SOURCE | IDENTIFIER |
|---|---|---|
| Deposited data | | |
| Data for this study | This study | Zenodo: https://doi.org/10.5281/zenodo.12607007 |
| All code for this study | This study | Github: https://github.com/gokselkeskin/adaptive-soaring-strategy |
| Software and algorithms | | |
| Python 3.9 | Python Software Foundation | https://www.python.org/ |
| Flight 1.25 | Pennycuick: Modelling the Flying Bird | https://booksite.elsevier.com/9780123742995/ |
| R | Free Software | https://www.r-project.org/ |

## EXPERIMENTAL MODEL AND STUDY PARTICIPANT DETAILS

### Datasets

GPS-tracking data recorded on freely flying birds allowed us to quantify the effects of morphology on flight performance and behavioural strategies and a direct comparison among different species. We collected an extensive dataset from research groups around the world studying thermalling birds in the wild (previously published and unpublished data sets), and carried out a comparative analysis of 12 bird species: Lesser Kestrel (*Falco naumanni*),[58] Peregrine falcon (*Falco peregrinus*),[32] Bald Eagle (*Haliaeetus leucocephalus*), Verreaux's eagle (*Aquila verreauxii*),[29] Tawny eagle (*Aquila rapax*), Steppe Eagle (*Aquila nipalensis*),[57] Eurasian Griffon vulture (*Gyps fulvus*),[35,36] Himalayan vulture (*Gyps himalayensis*),[35] Rüppell's Vulture (*Gyps Rüppellii*), Andean condor (*Vultur gryphus*), White stork (*Ciconia ciconia*),[54,73,74] Northern bald ibis (*Geronticus eremita*).[27]

## METHOD DETAILS

### Data preparation

Since the dataset was gathered from different devices and formats, we simplified the miscellaneous data in the same structure by taking only timestamp, longitude, latitude, and altitude recordings as the first step. The geodesic coordinates provided by the GPS were converted into metric coordinates using the locally flat approximation with an $(x, y) = (0, 0)$ origin at the beginning of data belonging to each bird and day. These coordinates were smoothed by a Gaussian filter, with window sizes adjusted according to the sampling rate of the GPS recordings (e.g., 5 points for 1 Hz, 50 points for 10 Hz) for each flight day of each individual in our custom Python codes. The filter applied a moving average centred on each data point, with a standard deviation of 0.8 to control the weight distribution within each window. Then we calculated the horizontal components of the velocity ($v_x$,$v_y$) and acceleration ($a_x, a_y$). High-frequency GPS tracks contain all movement of birds, from take-off to landing, and may include flapping flight. For this reason, thermalling and gliding flight parts of the track were automatically identified based on curvature ($\kappa = (v_x a_y - v_y a_x)/(v_x^2+v_y^2)^{1.5}$) and vertical speed ($v_z$) parameters (gliding: $|\kappa| < 0.01$ m$^{-1}$ and $v_z < 0$ m/s, thermalling: $|\kappa| > 0.01$ m$^{-1}$ and $v_z > 0$ m/s). Soaring occurred when birds made consecutive turns and when the average vertical ground speed was positive. Therefore, thermalling parts were identified as segments with positive vertical speeds and positive curvature. Since thermals drift with the wind, we removed the effects of wind effect (for details[32]) to obtain a more reliable estimate of circling radius. Thermalling parts lasting longer than ($t$ = 30 seconds) were defined as flying in thermal, and local wind velocity (speed and direction) was calculated using both horizontal components of the bird's velocity in the thermal as described in Ákos et al.[32] Additionally, this method allowed us to calculate daily average wind speed as $x$- and $y$-components.

### Evaluation of gliding and thermalling phases of flight

For each of these ascending phases, we determined circling radius, the mean instantaneous horizontal speed (circling velocity), the mean instantaneous vertical speed (climbing rate). Gliding is a type of flight when the birds fly forward and lose height (typically flying without flapping their wings, but even if they flap, they sink). So, we identified and extracted ''effective'' gliding parts using above mentioned thresholds for vertical speed and curvature that define the ''empirical'' polar curve that we use in this manuscript, and that is different from a traditional polar curve that defined for pure gliding. To estimate airspeed during gliding, we subtracted average daily wind velocity (speed and direction, see above) from ground speed during gliding. If no thermals were detected on a given day, as described above, we excluded that day from the analysis as in this study we focused on understanding the relationship between the behaviour during thermalling and gliding. Hereafter, all horizontal speed represents the estimated airspeed. The empirical polar curve

was fitted to the measured average sinking and horizontal velocities during gliding flight. We used a second-order approximation to capture the main characteristic of the curves and fitted $f(x) = ax^2 + bx + c$ for determining the empirical glide polar. We used these glide polars to identify the important gliding parameters of each species. The maximum glide ratio (the largest distance travelled from a given height) was calculated by drawing a tangent from the origin, or when the polar curve is approximated with a quadratic formula given above by $\sqrt{c/a}$. The speed at minimum sink airspeed was calculated by converting the quadratic function to vertex form, $f(x) = a(x - h)^2 + k$. Since the parabola is negative, the vertex represents the maximum point. The x-coordinate (the airspeed at minimum sink speed, $h$) is found using $-b/2a$, and the minimum sink speed (y-coordinate, $k$) is found by substituting the $h$ back into the original quadratic function. The airspeed at minimum sink ($v_{xy}^{Min\ Sink}$) denotes the horizontal speed at which the descent is minimum. When choosing a horizontal airspeed higher than $v_{xy}^{Min\ Sink}$, the rate of descent increases, but this increment is initially modest, causing the glide ratio – the ratio of forward speed to descent – to keep rising. The glide ratio reaches its peak at the best-glide airspeed ($v_{xy}^{Best\ Glide}$). Above this critical value, the glide ratio steadily declines.

## Cross-country strategy

Selection of inter-thermal gliding speed affects the overall cross-country speed which is the ratio between the distance travelled during gliding divided by the total time (that includes both gliding and thermalling). By optimally selecting the inter-thermal gliding speed birds (and any aircrafts) can maximise the distance covered within the same amount of time, which is an essential factor during migration for migratory birds or during long-ranging foraging flights (searching for prey or carrion efficiently) for birds of prey and scavengers. To study the effect of thermal strength on inter-thermal horizontal speed, we selected species from our data set, which had multiple days to present large enough range for a linear fit. We selected species that had at least 10 different daily flight trajectories (allowing data coming from multiple individuals).

We used a linear approximation to represent the relationship between horizontal speed during inter-thermal flight, $v_{xy}$, and climb speed, $v_{climb}^{Thermal}$ (that relates to the strength of the thermals). Before fitting a line, we removed the outliers using Gaussian distribution and cut-off from two standard deviations. We estimated the observed strategy by fitting a line ($f(x) = Ax + B$) using the horizontal glide airspeed ($v_{xy}$) as $f(x)$ that is the result of the bird's decision-making, and the climb speed ($v_{climb}^{Thermal}$) as $x$ that is the input variable for the optimization. Here, parameter $A_{\text{Observed}}$ shows how adaptively the birds tune their inter-thermal speed to the climb speed, and a fit with $A_{\text{Observed}} = 0$ would indicate that the birds use the same inter-thermal speed irrespective of thermal strength. Birds with high values of $A_{\text{Observed}}$ fly between thermals much faster on days with strong thermals as opposed to weak thermals, while birds with $A_{\text{Observed}}$ close to zero do not vary their inter-thermal speed based on thermal strength. The intercept of that line, $B_{\text{Observed}}$, captures the preferred gliding speed in zero thermal conditions, representing the lowest value for daily average horizontal speed during gliding flight, thus we name it as *preferred no-thermal gliding speed* (which is the horizontal component).

## Generating a theoretical glide polar using the Pennycuick's flight tool

We used Pennycuick's Flight tool version 1.25[13] to generate theoretical glide polars based on the morphological parameters. We set environment and aerodynamics parameters to remain consistent across all species to demonstrate morphology-related differences. All glide polars were created in the environmental conditions at an altitude of 1400 metres (highest mean altitude among all species), and at the respective air density, 1.069 kg/m$^2$. The wingspan reduction law was configured to 'minimise induced + profile drag,' effectively flattening the glide polar at higher speeds. We initially generated the glide polars using the default settings of the software, which only differed in the induced drag factor (0.9). Later, we employed the value for the same parameter found in the Modelling Flying Bird (1.1). In order to obtain more accurate estimations for the glide polars, we conducted literature research on body and wing profile drag coefficients from experimental studies.[48,49,75,76] From the newest wind tunnel research,[49] we found a value of 0.25 for the body drag coefficient and 0.025 for the wing profile drag coefficient by averaging the given range for the swift (*Apus apus*). These updates on the drag coefficients allowed us to create closer glide polars to our empirical glide polars.

## Phylogenetic analysis

We employed phylogenetic generalized least-squares regressions (PGLS)[77,78] to assess the effect of evolutionary relatedness on the data, using 1000 phylogenetic trees provided by Birdtree.org, based on the Ericson phylogeny as the backbone.[79] To focus on the species relevant to our analysis, we constructed a phylogenetic subtree containing only the 12 species used in this study. Using the function keep.tip from the R package phytools,[80] we have pruned all the trees mentioned above. This approach ensured that the phylogenetic relationships among the selected species were preserved, while unnecessary lineages were excluded from the analysis. Since we have two datasets from Griffon vultures, we could not include both in the PGLS analysis. Therefore, we selected the $Gf_2$ Griffon vulture dataset, which had more data points (Table S1), for the regression models.

To ensure stable estimation of the phylogenetic signal ($\lambda$) and improve numerical optimization during PGLS, we rescaled the branch lengths of the phylogenetic tree using Grafen's method.[81]

We estimated Pagel's $\lambda$ through maximum likelihood optimization[77,78] to measure the influence of evolutionary history on the data. The 'ape', 'phytools' and 'caper' packages for R[80,82,83] were used for the analyses. PGLS regression was performed utilizing each tree individually, and the average was taken from the resulting coefficients.

## QUANTIFICATION AND STATISTICAL ANALYSIS

### Randomization test

We applied a randomization test (see e.g.,[84]), which presents a methodology for evaluating the significance of linear relationships between variables. This approach entails maintaining the independent variable (x) constant while permuting the dependent variable (y) numerous times. By fitting a linear model and assessing the goodness of fit, typically measured through R-squared, determination coefficient ($R^2$) metrics in our results, for the couples in each iteration, an empirical null distribution was built. Consequently, this enabled the determination of the extent to which the observed association between x and y deviates from what would be expected under random chance alone, yielding a reliable p-value for the significance of the linear relationship.